Supporting Information

The Mammalian Neuronal Sodium Channel Blocker μ-Conotoxin BuIIIB has a Structured N-terminus that Influences Potency

Zhihe Kuang,[†,‡] Min-Min Zhang,[§] Kallol Gupta,[‖] Joanna Gajewiak,[#] Jozsef Gulyas,[++] Padmanabhan Balaram, [‖] Jean E. Rivier, [++] Baldomero M. Olivera,[#] Doju Yoshikami,[#] Grzegorz Bulaj, [#] and Raymond S. Norton *[,¶]

[‡] The Walter and Eliza Hall Institute of Medical Research, 1G Royal Parade, Parkville, Victoria, 3052, Australia

[§] Department of Biology, University of Utah, Salt Lake City, Utah 84112, United States

[‖] Molecular Biophysics Unit, Indian Institute of Science, Bangalore, 560 012, India

[++] The Clayton Foundation Laboratories for Peptide Biology, The Salk Institute for Biological Studies, 10010 North Torrey Pines Road, La Jolla, CA 92037, United States

[#] Department of Medicinal Chemistry, College of Pharmacy, University of Utah, Salt Lake City, Utah 84108, United States

[¶] Medicinal Chemistry, Monash Institute of Pharmaceutical Sciences, Monash University, Parkville, Victoria, 3052, Australia

[†] Institute of Biomedicine, Guangzhou 510632, China

[*] **Corresponding Author** ray.norton@monash.edu

RESULTS

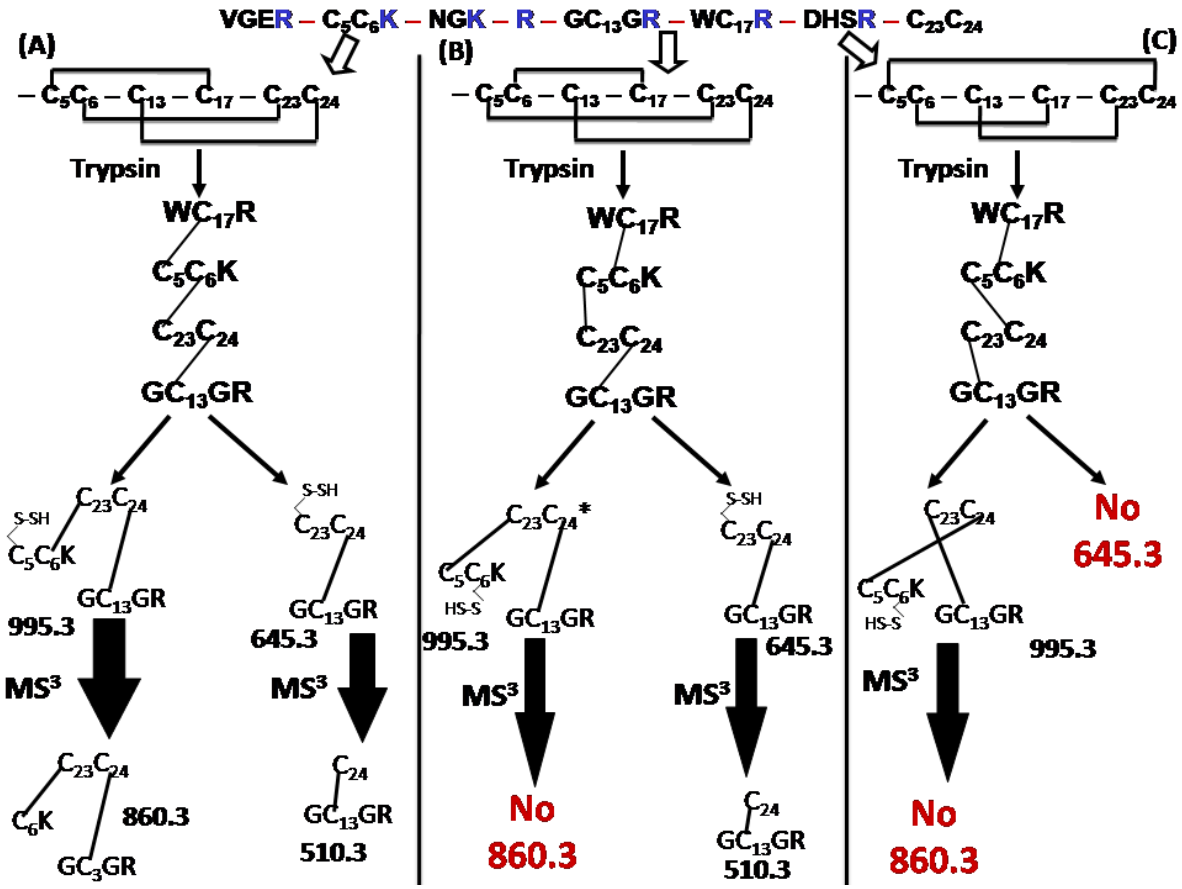

Figure S1. Diagnostic ions for the disulfide pairing scheme of μ-BuIIIB and the feasibility of the same for the other two observed disulfide pairing schemes of μ-conotoxins.

.

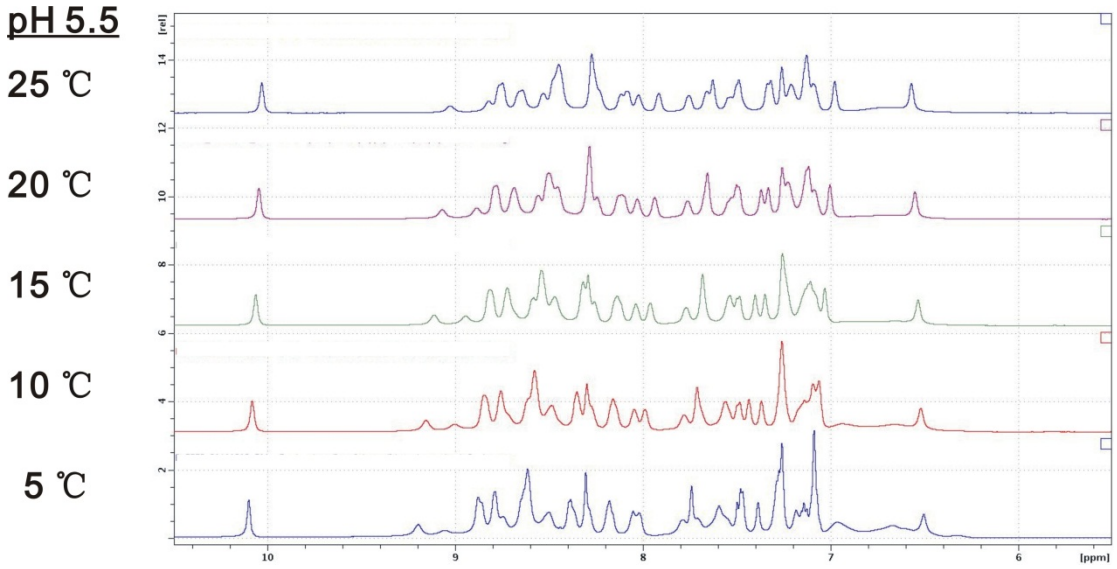

Figure S2A. Amide and aromatic region of 1D ^{1}H-NMR spectra of μ-BuIIIB at 5 °C intervals from 5 to 25 °C at pH 5.5, acquired on a DRX-600 spectrometer.

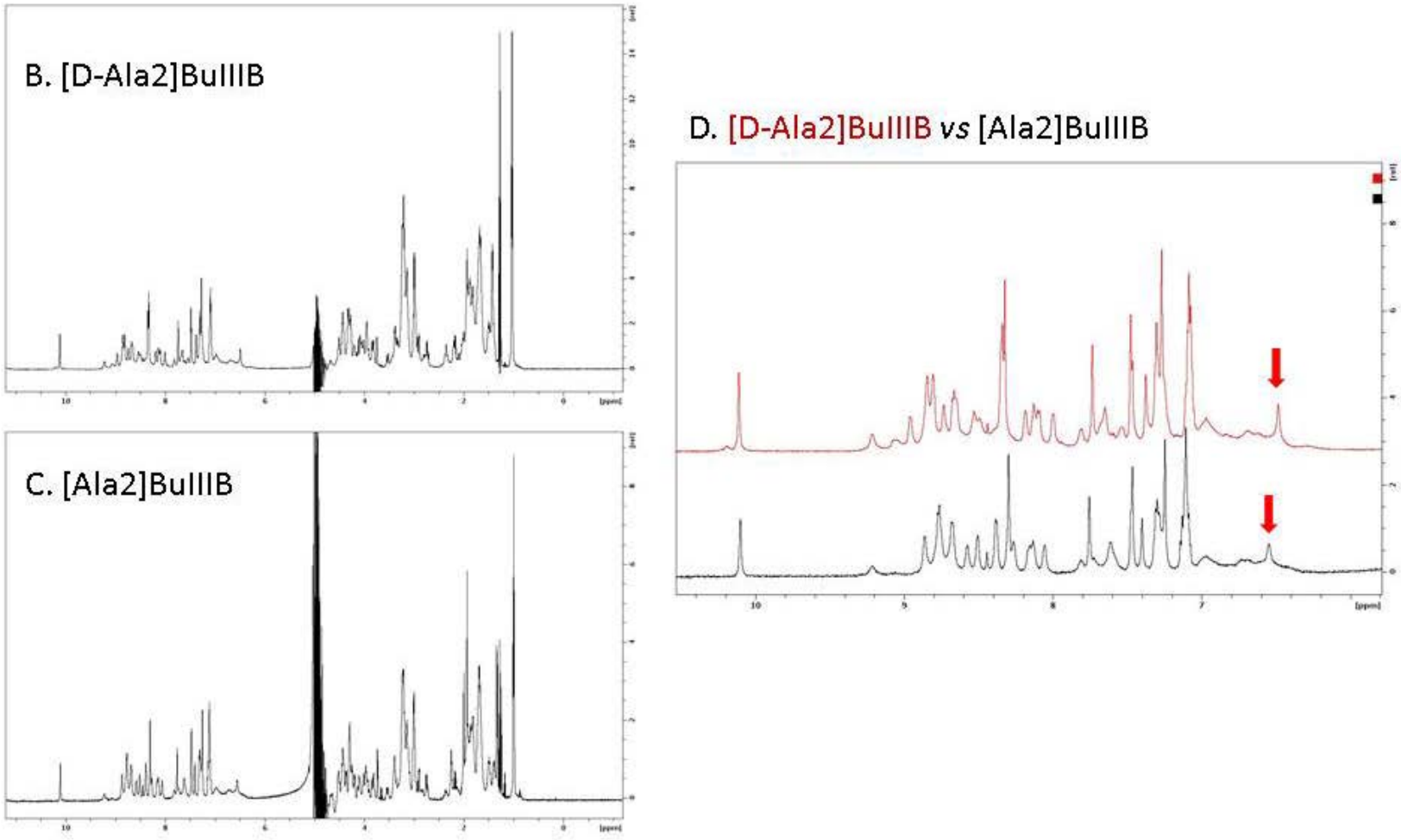

Figure S2B-C. 1D ^{1}H-NMR spectra of [D-Ala2]BuIIIB and [Ala2]BuIIIB at 5 °C and pH 5.6, acquired using an excitation pulse sequence on a Bruker Avance 600 spectrometer. Their similarity to spectra of μ-BuIIIB confirms the correct folding of these analogs and documents their purity. The expanded views of the amide and aromatic regions of these spectra are very similar to those of μ-BuIIIB in Figure S2A; in particular, the shifted His20 resonance indicated by the red arrow is a marker of the native fold.

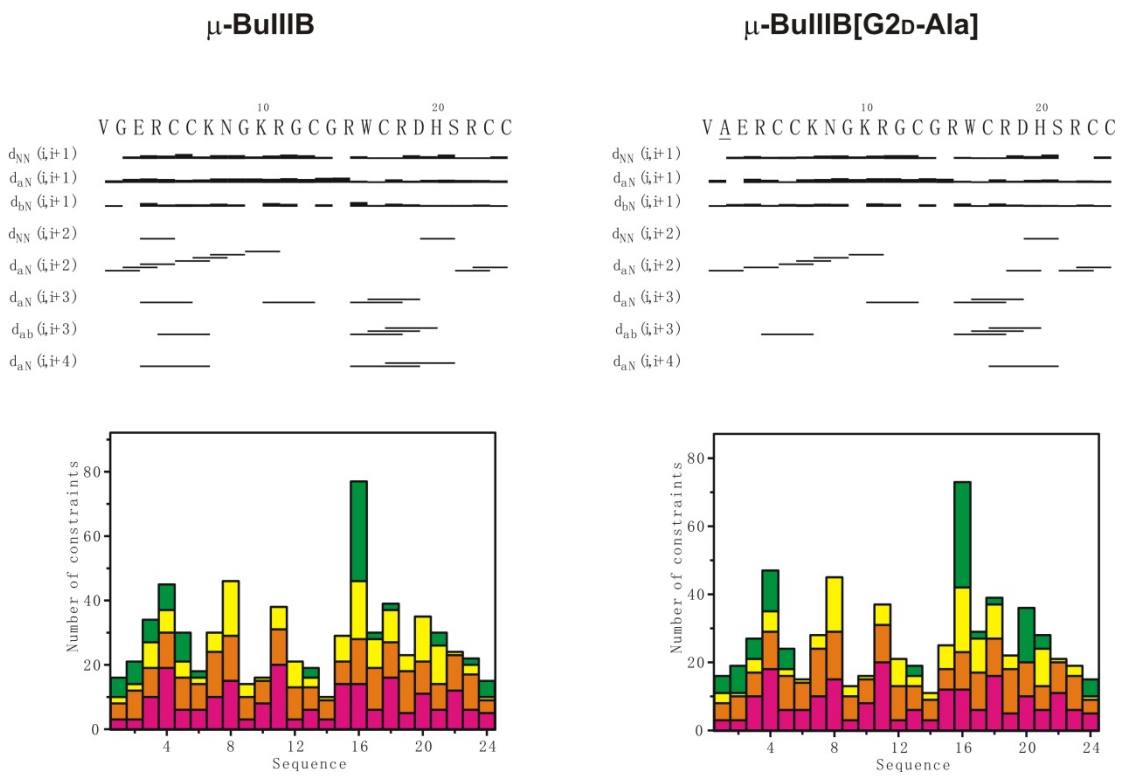

Figure S3. NOE connectivities and statistics for μ-BuIIIB and [D-Ala2]BuIIIB. Top panels summarize the sequential and medium-range NOEs connectivities. Bottom panels indicate the numbers of intra-residue (pink), sequential (orange), short range (2≤i-j≤5, yellow), and long range (i-j>6, green) NOE constraints used in the final structure calculations. These figures were prepared using CYANA 2.1. Supp(*1*)

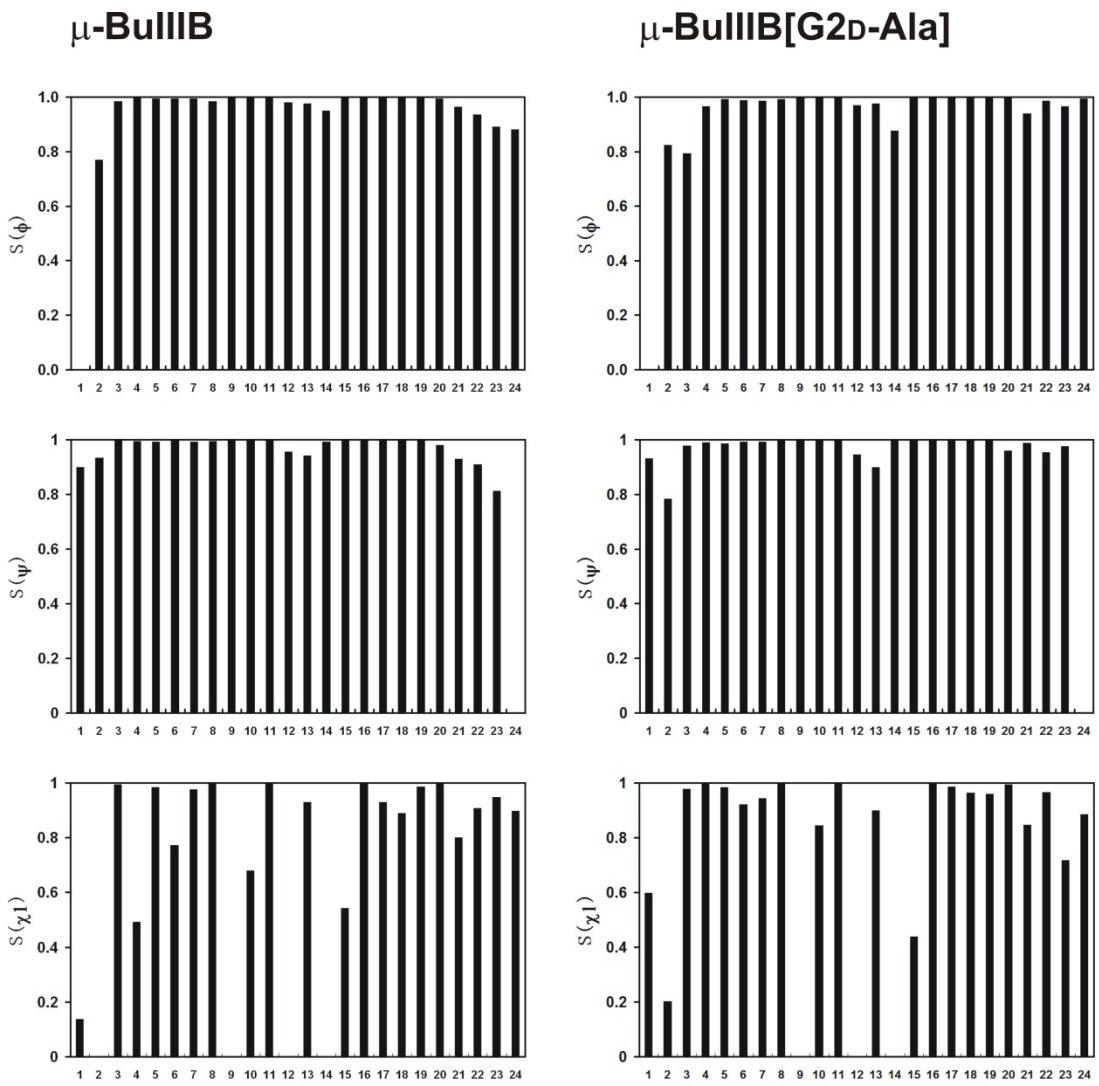

Figure S4. Angular order parameters (S) for backbone (φ, ψ) and sidechain (χ^1) dihedral angles of μ-BuIIIB and [D-Ala2]BuIIIB plotted against residue number. These parameters were calculated using MOLMOL. Supp(*2*)

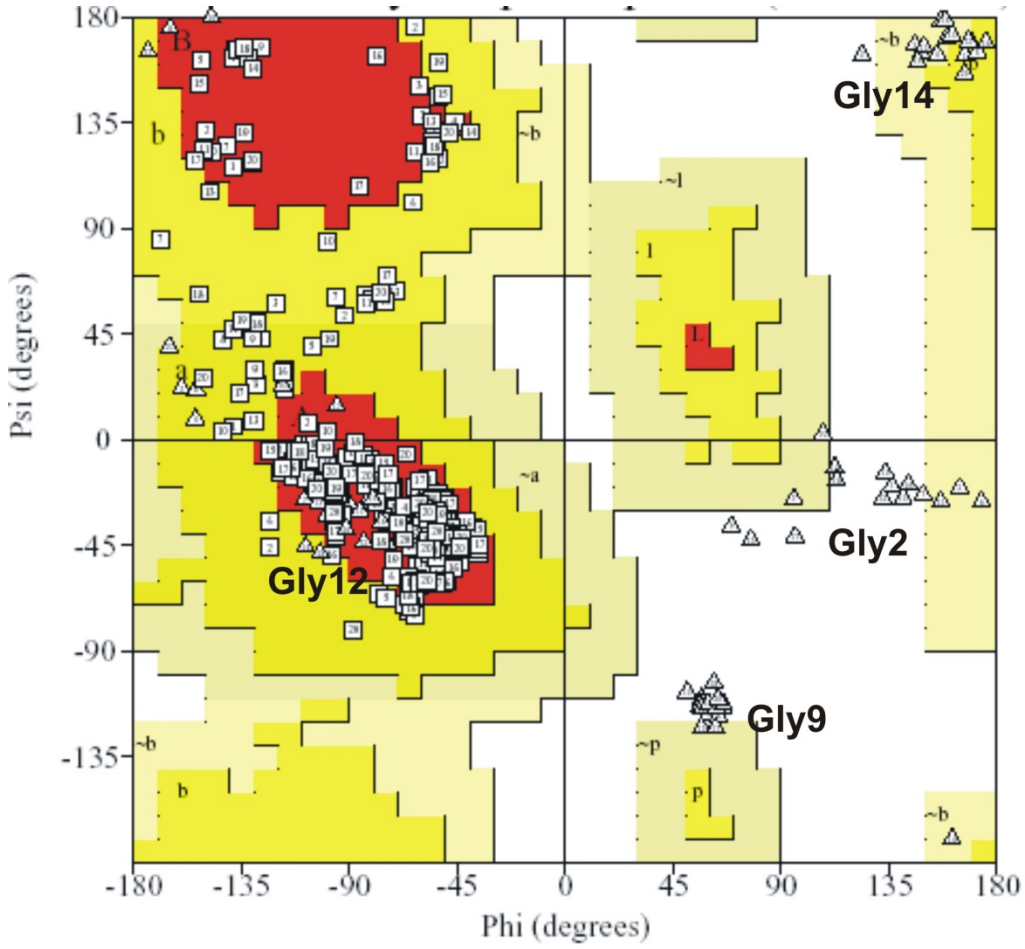

Figure S5. Ramachandran plot of the final 20 structures of μ-BuIIIB. Plots for Gly residues are labeled. This figure was prepared using PROCHECK-NMR. Supp(*3*)

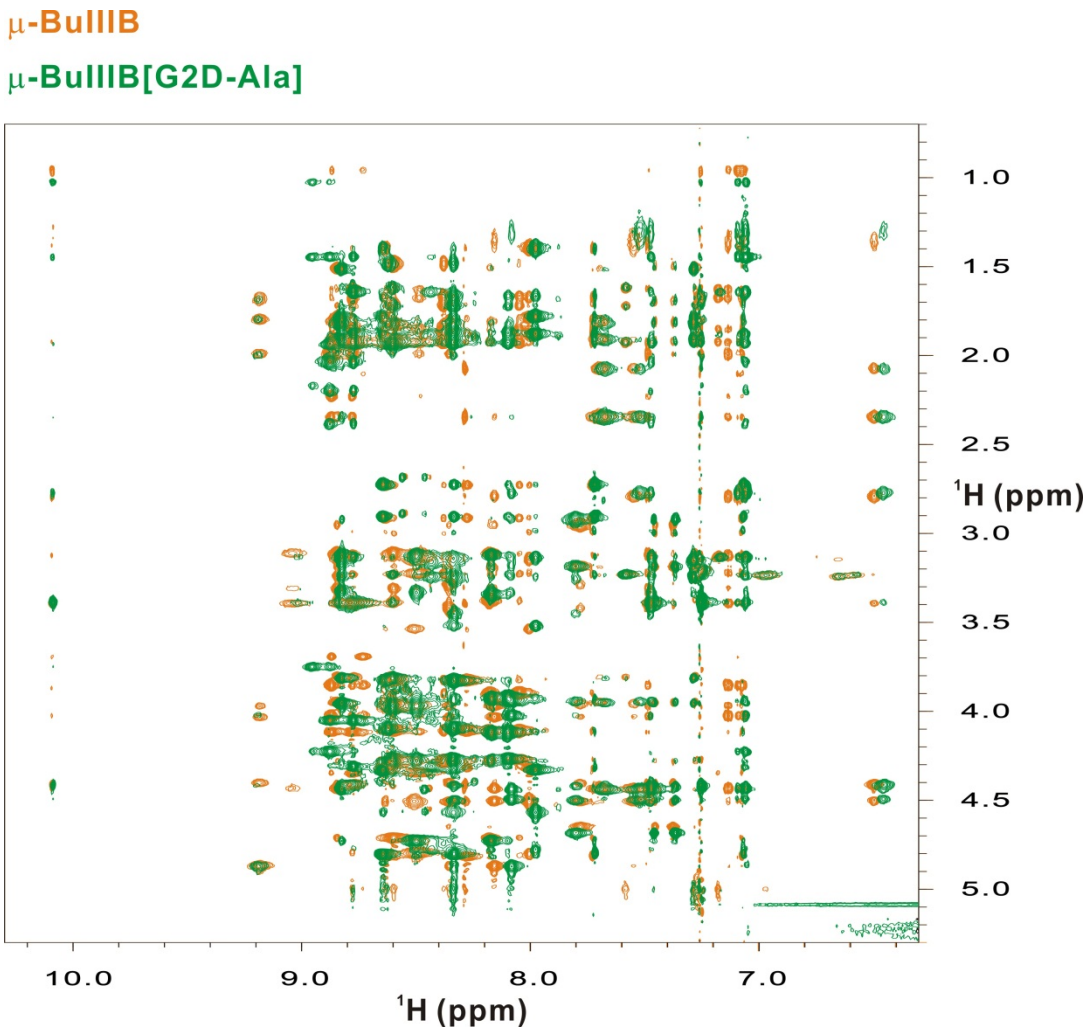

Figure S6. Overlay of the amide and aromatic regions of 2D NOESY spectra of μ-BuIIIB (orange) and [D-Ala2]BuIIIB (green). These spectra were recorded at 5 °C and pH 5.5 on an Avance-800 spectrometer with a TCI cryoprobe.

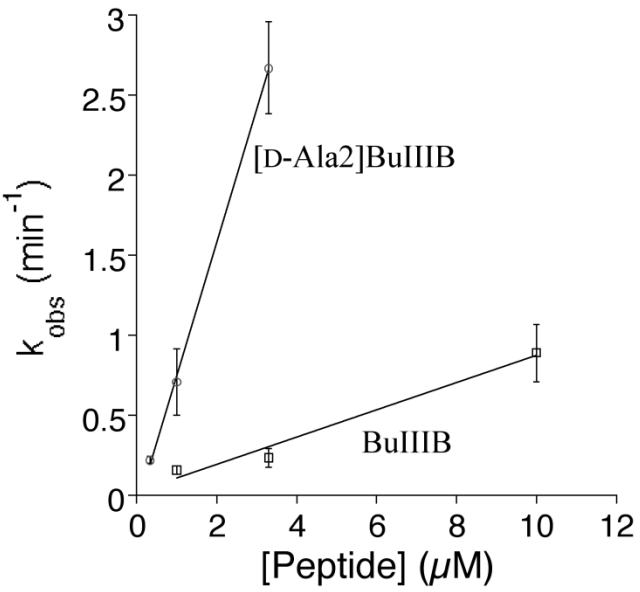

Figure S7. Rate of block of sodium current as a function of peptide concentration. The observed rate of block, k_{obs}, was obtained as described in Methods by curve fit of the onsets of block such as those shown in Figures 6B and D. The slopes of the curves, obtained by linear regression (see lines), yielded the k_{on} values listed in Table 2.

Table S1. Block of rodent $Na_V1.3$, $Na_V1.4$, $Na_V1.6$ and $Na_V1.7$ by μ-BuIIIB or [D-Ala2]BuIIIB[a]

Peptide	rNa$_V$1.3			rNa$_V$1.4			mNa$_V$1.6			rNa$_V$1.7		
	k_{on} ($\mu M \cdot min)^{-1}$	k_{off} (min^{-1})	K_d (μM)	k_{on} ($\mu M \cdot min)^{-1}$	k_{off} (min^{-1})	K_d (μM)	k_{on} ($\mu M \cdot min)^{-1}$	k_{off} (min^{-1})	K_d (μM)	k_{on} ($\mu M \cdot min)^{-1}$	k_{off} (min^{-1})	K_d (μM)
μ-BuIIIB	0.085 ± 0.010	0.017 ± 0.007	0.20 ± 0.09	4.2 ± 0.8	0.015 ± 0.005	0.0036 ± 0.0014	0.090 ± 0.014	0.14 ± 0.02	1.55 ± 0.36	NA[b]	NA[b]	>300 μM[b]
[D-Ala2] BuIIIB	0.83 ± 0.050	0.0040 ± 0.0017	0.0048 ± 0.0020	9.0 ± 0.9	0.0031 ± 0.0014	0.00034 ± 0.00016	0.24 ± 0.03	0.10 ± 0.03	0.42 ± 0.13	0.041 ± 0.008	0.21 ± 0.01	5.1 ± 1.0
Ratio K_d μ-BuIIIB/K_d[D-Ala2] BuIIIB			41.7			10.6			3.7			> 59

[a]Prefixes for Na_V1 clones are "r" for rat and "m" for mouse. Values represent mean ± SD, obtained as described in Materials and Methods and Table 2. Data for μ-BuIIIB are from Wilson et al. *(20)*.

[b]At the highest concentration tested (30 mM), μ-BuIIIB blocked < 10% of the sodium current of $rNa_V1.7$; therefore, k_{on} and k_{off} could not determined and K_d was estimated assuming the Langmuir binding isotherm, fraction blocked = $1/(1 + (K_d/[\mu\text{-BuIIIB}]))$.

METHODS

Peptide Synthesis, Purification and Characterization. Peptides were synthesized by t-Butoxycarbonyl (Boc) solid phase methodology on a CSBio Peptide synthesizer (Model CS536) utilizing 4-methylbenzhydrylamine resin as solid support. Amino acid derivatives Boc-Ala-OH, Boc-Asn(xanthyl)-OH, Boc-Asp(cyclohexyl ester)-OH, Boc-Arg(tosyl)-OH, Boc-Cys(4-methoxybenzyl)-OH, Boc-Gly-OH, Boc-Glu(cyclohexyl ester), Boc-His(DNP)-OH, Boc-Lys(2-chlorobenzyloxycarbonyl)-OH, Boc-Ser(benzyl)-OH, Boc-Trp-OH, and Boc-Val-OH were obtained from Bachem Inc., Chem-Impex International, Novabiochem, Reanal, and AApptec. All solvents were reagent grade or better.

Four equivalents of Boc-amino acid (2.2 mmol) based on the original substitution of the 4-methylbenzhydrylamine resin (0.54 mmol/ g) was used for each coupling. Peptide couplings were mediated by N, N'-diisopropylcarbodiimide/1-hydroxy-benzotriazole (2.1 mmol/ 4.2 mmol) in N-methylpyrrolidone (NMP) for 1 h. Boc removal was achieved with trifluoroacetic acid (TFA) (containing 1–2% m-cresol) for 15 min. A methanol wash followed TFA treatment and then successive washes with triethylamine solution (10% in NMP), methanol, and CH_2Cl_2 completed the neutralization sequence. After completion of the synthesis and removal of the DNP group of the side chain of His with 20% of thiophenol in NMP for 3 h and the Boc group of the peptide's final amino group with TFA, the peptides were deprotected and cleaved from the resin by anhydrous HF containing the scavengers anisole (10% v/v) and methyl sulfide (5% v/v) for 90 min at 0°C. The cold diethyl ether-precipitated crude non-cyclized peptides were purified using a preparative Shimadzu RP-HPLC system (two Shimadzu LC 8A pumps, an SCL-10A controller, and an SDP 10A UV detector), a 5 x 30 cm cartridge packed in our laboratory with reversed-phase 300 Å Vydac C_{18} silica (15-20 μm particle size) and the solvent system 0.1% TFA/ H_2O/ CH_3CN. The peptides eluted with a flow rate of 100 mL/min. A linear gradient 1% B per 1 min increases from the baseline %B (eluent A = 0.1 % TFA/ H2O, eluent B = 60% CH_3CN, 40% A) was applied. Analytical HPLC screening was performed on a Vydac C18 column (0.46 x 25 cm, 5 μm particle size, 300 Å pore size) connected to a Rheodyne injector, and a Shimadzu analytical HPLC system (two Shimadzu LC 10AT pumps, an SCL-10A controller, and an SDP 10A UV detector). Fractions containing the right product were pooled and folded.

Folding was achieved in 700 mL of 4% ammonium-acetate (NH_4Ac) buffer (pH 6.8, containing 1 M NaCl) by air oxidation. The solution was stirred slowly at room temperature for several days till the Ellmann-test(*41*) indicated no free SH group present in the solution.

After folding, the products were purified further by preparative RP-HPLC using a linear gradient 0.3 % B per 1 min increase from the baseline %B (eluent A = triethylammonium phosphate at pH 2.25, eluent B = 60% CH_3CN, 40% A) in the first purification step. Out of the different folded conformers, peptides that eluted first from the column with the lowest %B buffer concentration were collected and desalted in a second purification step on the same column using a linear gradient 1% B per 1 min increases from the baseline %B (eluent A = 0.1% TFA, eluent B = 60% CH_3CN, 40% A). Analytical HPLC traces for the crude reduced, crude oxidized, and purified oxidized peptides are shown in Supplementary Figures S8-S10 (for [Ala2]BuIIIB), S11-

S13 ([D-Ala2]BuIIIB), and S14-S16 (μ-BuIIIB).

Analytical HPLC was performed on a Phenomenex Kinetex XB C18 column (0.46 x 15 cm, 2.6 μm particle size) using a Shimadzu analytical HPLC system (two Shimadzu LC 10AT pumps, an SCL-10A controller, and an SDP 10A UV detector). A linear gradient 1% B/min increased from 0%B to 50%B (Eluent A = 0.05% TFA/H_2O, Eluent B = 0.05% TFA/CH3CN) at a flow rate of 1.2 mL/min. Detection was at 210 nm. Other analogs not shown were folded and purified similarly to those shown below.

Masses (MALDI-MS) were measured on an ABI-Perseptive DE-STR instrument. The observed monoisotopic (M+H)+ values of the peptides corresponded with the calculated (M+H)+ values as follows: [Ala1]BuIIIB $[M+H]_{calc}$ = 2734.15 $[M+H]_{obs}$ = 2734.09; [D-Ala2]BuIIIB $[M+H]_{calc}$ = 2776.19 $[M+H]_{obs}$ = 2776.42; [Ala3]BuIIIB $[M+H]_{calc}$ = 2704.14 $[M+H]_{obs}$ = 2704.68; [Ala4]BuIIIB $[M+H]_{calc}$ = 2677.11 $[M+H]_{obs}$ = 2677.30; [des1-4]BuIIIB $[M+H]_{calc}$ = 2320.94 $[M+H]_{obs}$ = 2320.64

Mass Spectrometry. The mass spectrometric experiments to determine the disulfide connectivity were performed on a Bruker HCT Ultra ETDII ion trap mass spectrometer. All experiments were performed through LC-MS analysis of the samples by coupling the ion trap mass spectrometer with an Agilent 1100 HPLC system. The peptide samples were subjected to LC-MS using a reverse phase C18 analytical column, with H_2O/ acetonitrile (with 0.1% formic acid) as the solvent system, at a flow rate of 0.2 mL/min. The CID experiment was performed by selecting the precursor ion and subsequently fragmenting it through collision with He gas. The fragmentation amplitude (*V*p−p) was kept between 1 and 3. The spectra were averaged over four scans. The program DisConnect,*(26)* used for mass spectral annotation, can be downloaded from http://mbu.iisc.ernet.in/~pbgrp/DisConnect.htm.

NMR spectroscopy - NMR experiments were recorded on a 2.6 mM sample of μ-BuIIIB in 95% H_2O/5% ^2H_2O at pH 5.5. A series of one-dimensional (1D) spectra at 5 °C intervals was collected over the temperature range of 5-25 °C. Data for structure calculations were then collected at 5 °C. A two-dimensional (2D) homonuclear total correlation (TOCSY) spectrum with a spin-lock time of 70 ms, and double-quantum-filtered correlated spectroscopy (DQF-COSY) spectrum were acquired on a DRX-600 spectrometer equipped with a triple-resonance probe. 2D nuclear Overhauser enhancement (NOESY) spectra with mixing times of 50 and 250 ms were recorded on an Avance-800 spectrometer equipped with a TCI cryoprobe. ^{15}N-HSQC, and ^{13}C-HSQC spectra were recorded on an Avance-500 spectrometer equipped with a TXI cryoprobe. NMR experiments of a 1.2 mM [D-Ala2]BuIIIB sample were performed at pH 5.5 and 5 °C. 2D TOCSY was acquired on a DRX-600 spectrometer. 2D NOESY (250 ms), ^{15}N-HSQC, and ^{13}C-HSQC spectra were recorded on an Avance-800 spectrometer with a TCI cryoprobe. Spectra were processed using TOPSPIN version 1.3 (Bruker Biospin) and analysed using XEASY. Supp(*4*)

Structural Constraints. Backbone and side-chain ^{1}H, ^{13}C, and ^{15}N chemical shifts of μ-BuIIIB

were assigned. NOEs were assigned automatically using CYANA 2.1. Supp(*5*) Because the [D-Ala2]BuIIIB analog only exhibited minor chemical shift alternations compared to μ-BuIIIB (see below), NOEs of [D-Ala2]BuIIIB were readily assigned based on the μ-BuIIIB assignments. φ and ψ angle constraints were predicted using TALOS+ Supp(*6*) based on chemical shifts of N, H^{α}, C^{α} and C^{β} atoms and combined with an analysis of $^{3}J_{HNH\alpha}$ coupling constants of μ-BuIIIB based on DQF-COSY spectrum. Glycine residues were not restrained in structure calculations for both peptides. For μ-BuIIIB, χ^{1} angles of some residues were determined on the basis of analysis of a short mixing time (50 ms) NOESY spectrum. Two χ^{1} angles (His20, Cys23) were constrained in the final structure calculations for μ-BuIIIB but none in structure calculations for [D-Ala2]BuIIIB.

Structure Calculations. Families of 200 structures was calculated using Xplor-NIH Supp(*7*) for μ-BuIIIB and [D-Ala2]BuIIIB, respectively, using standard simulation annealing scripts. The 80 lowest-energy structures were then subject to energy minimization in water; during this process, a box of water with a periodic boundary of 18.856 Å was built around the peptide structure and the ensemble was energy-minimized on the basis of NOE and dihedral constraints and the geometry of the bonds, angles, and impropers. Supp(*8*) From this set of structures, a final family of 20 lowest-energy structures were chosen for analysis using PROCHECK-NMR Supp(*3*) and MOLMOL. Supp(*2*) The final structures had no experimental distance violations greater than 0.2 Å or dihedral angle violations greater the 5°. Structural figures were prepared using MOLMOL(*2*) and PyMOL (DeLano, 2004; http://pymol.sourceforge.net).

Oocyte Electrophysiology. Oocytes expressing $Na_V1.3$, $Na_V1.4$, $Na_V1.6$ or $Na_V1.7$ were prepared and voltage-clamped essentially as previously described.(*17, 20*) Supp(*9*) Na_V1 isoforms were not co-expressed with $Na_V\beta$ subunits so results could be compared directly with those obtained previously.(*20*) Briefly, a given oocyte was injected with ~30 nL cRNA of rat $Na_V1.3$ (15 ng), rat $Na_V1.4$ (0.6 ng), mouse $Na_V1.6$ (30 ng) or rat $Na_V1.7$ (15 ng), and incubated 1 to 2 days at 16 °C in ND96 composed (in mM) of: NaCl (96), KCl (2), $CaCl_2$ (1.8) $MgCl_2$ (1), and HEPES (5), pH 7.5. The incubation medium also contained the antibiotics penicillin (100 units/mL), streptomycin (0.1 mg/mL), amikacin (0.1 mg/mL), and Septra (0.2 mg/mL). Oocytes in ND96 were two-electrode voltage-clamped using microelectrodes containing 3M KCl (<0.5 MΩ) and held a membrane potential of –80 mV. Sodium channels were activated by stepping the potential to –10 mV for 50 ms every 20 sec. Current signals were filtered at 2 KHz, digitized at a sampling frequency of 10 KHz, and leak-subtracted by a P/8 protocol using in-house software written in LabVIEW (National Instruments, Austin, TX).

The oocyte-recording chamber consisted of a well (4 mm diameter, 30 μL volume) fabricated from the silicone elastomer, Sylgard (Dow Corning, Midland MI). Oocytes were exposed to toxin by applying 3 μL of toxin at 10-times its final concentration with a pipettor and manually stirring the bath for a few seconds by gently aspirating and expelling a few μL of the bath fluid several times with the pipettor. Toxin exposures were in a static bath to conserve material. Toxin-containing solution was washed out of the well by perfusion with ND 96, initially at a

speed of 1.5 mL/min for ~20 s, then at 0.5 mL/min thereafter. Recordings were made at room temperature.

Data Analysis. The observed rate constant, k_{obs}, was obtained by fitting the time course of block of the peak sodium current with a single exponential function. The on-rate constant, k_{on}, was determined from the slope, obtained by linear regression, of the plot of k_{obs} *versus* [toxin],(*14*) assuming the equation for a bimolecular reaction between ligand and its receptor, $k_{obs} = k_{on}[ligand] + k_{off}$. Supp(*10*) The off-rate constants, k_{off} of μ-BuIIIB and its analogs with $Na_V1.6$ and $Na_V1.7$ were determined by fitting the time course of recovery from block following toxin washout to a single-exponential function. However, the time courses of recovery with $Na_V1.3$ and $Na_V1.4$ were too slow for accurate determination of k_{off} by the preceding procedure; instead, they were estimated in each case from the level of recovery following 20 min of wash assuming an exponential rate of recovery (longer times were not used to avoid errors introduced by possible base-line drift).(*29*) The value for each data point in the table and plots represents the mean ± SD ($N \geq 3$ oocytes). Curve fittings were done with KaleidaGraph (Synergy Software, version 4.1) and Prism (GraphPad Software, version 5.0).

Figure S8. Analytical HPLC of crude reduced [Ala2]BuIIIB (see text for details).

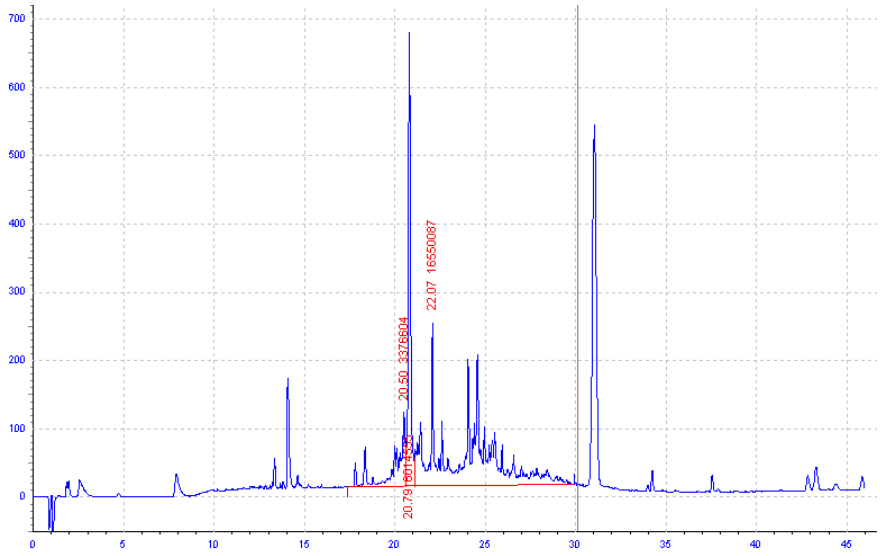

Figure S9. Analytical HPLC of crude oxidized [Ala2]BuIIIB (see text for details).

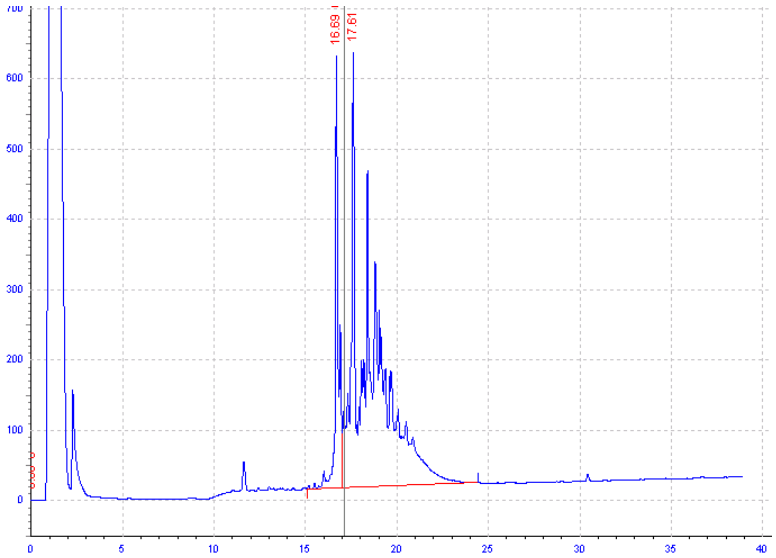

Figure S10. Analytical HPLC of purified oxidized [Ala2]BuIIIB (see text for details).

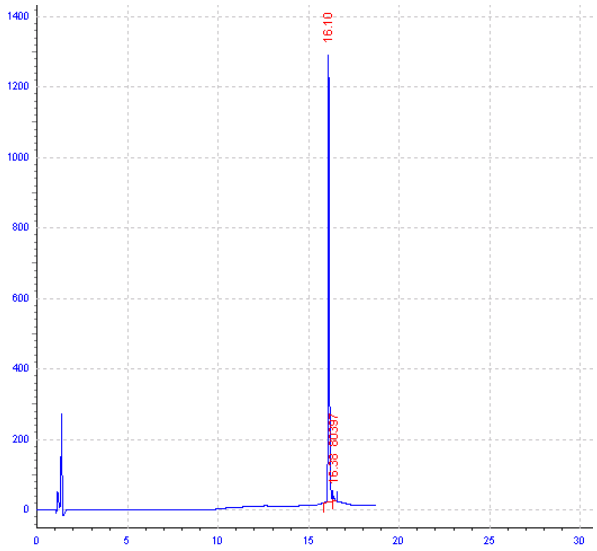

Figure S11. Analytical HPLC of crude reduced [DAla2]BuIIIB (see text for details).

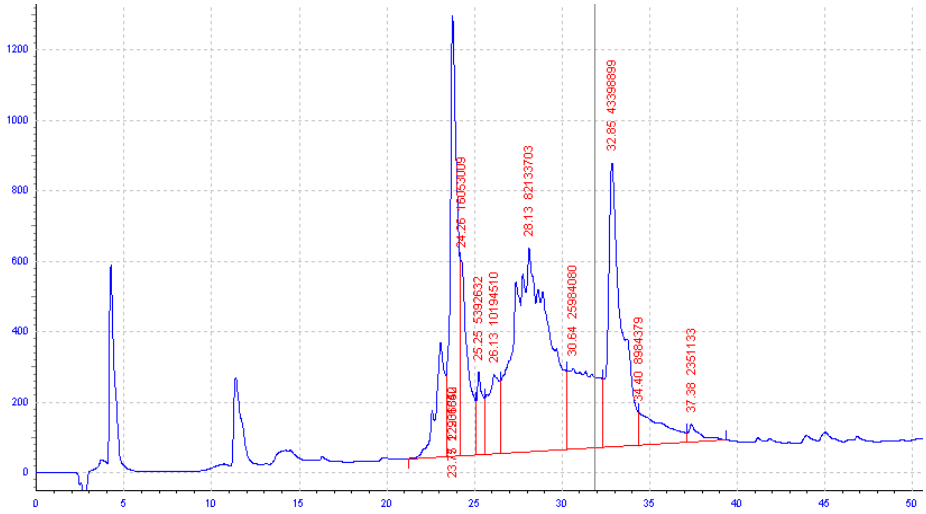

Figure S12. Analytical HPLC of crude oxidized [D-Ala2]BuIIIB (see text for details).

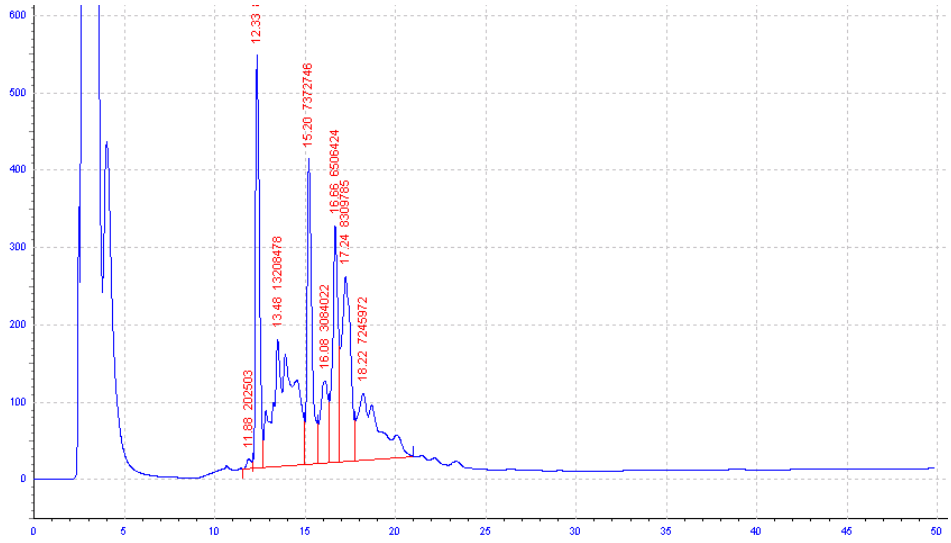

Figure S13. Analytical HPLC of purified oxidized [D-Ala2]BuIIIB (see text for details).

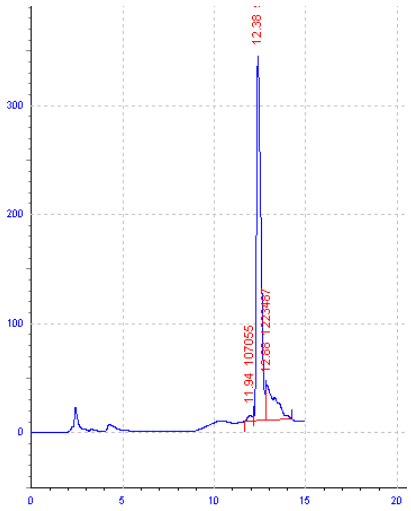

Figure S14. Analytical HPLC of crude reduced µ-BuIIIB (see text for details).

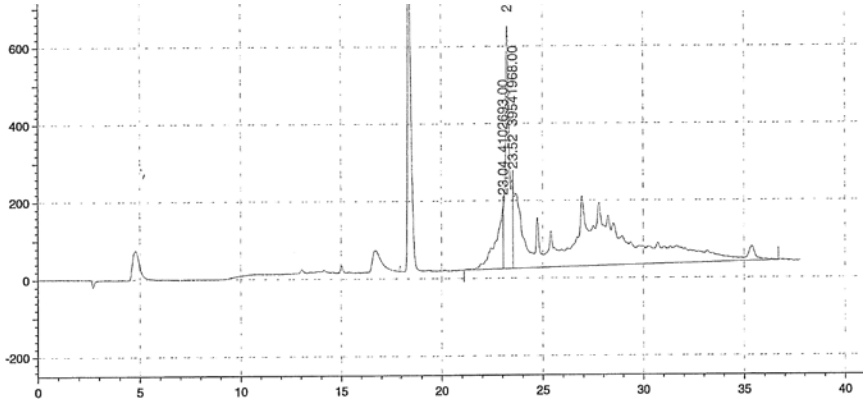

Figure S15. Analytical HPLC of crude oxidized µ-BuIIIB (see text for details).

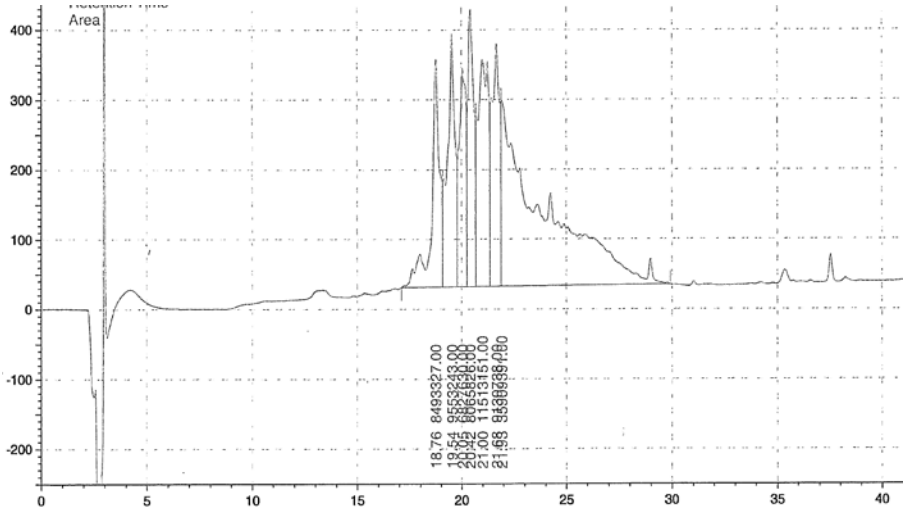

Figure S16. Analytical HPLC of purified oxidized µ-BuIIIB (see text for details).

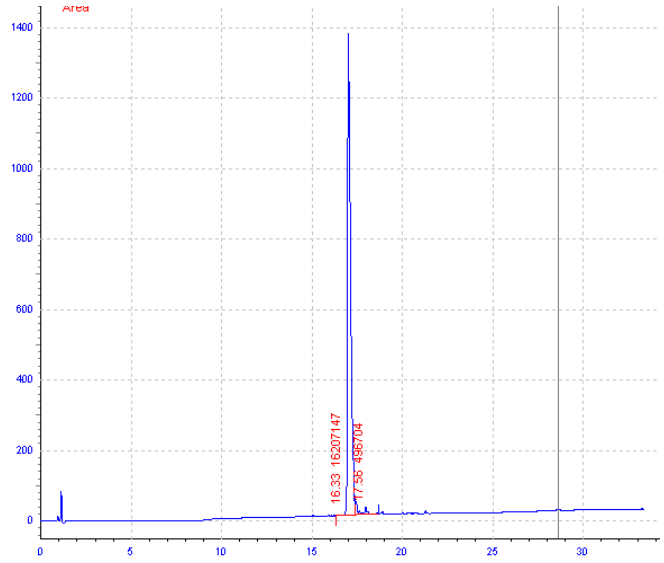

References (note that references that occur exclusively in the Supporting Information are preceded by Supp)

1. Güntert, P., Mumenthaler, C., and Wüthrich, K. (1997) Torsion angle dynamics for NMR structure calculation with the new program DYANA, *J Mol Biol 273*, 283-298.
2. Koradi, R., Billeter, M., and Wüthrich, K. (1996) MOLMOL: a program for display and analysis of macromolecular structures, *J Mol Graph 14*, 51-55, 29-32.
3. Laskowski, R. A., Rullmannn, J. A., MacArthur, M. W., Kaptein, R., and Thornton, J. M. (1996) AQUA and PROCHECK-NMR: programs for checking the quality of protein structures solved by NMR, *J Biomol NMR 8*, 477-486.
4. Bartels, C., Xia, T., Billeter, M., Guntert, P., and Wüthrich, K. (1995) The program XEASY for computer-supported NMR spectral-analysis of biological macromolecules, *J Biomol NMR 6*, 1-10.
5. Herrmann, T., Guntert, P., and Wüthrich, K. (2002) Protein NMR structure determination with automated NOE assignment using the new software CANDID and the torsion angle dynamics algorithm DYANA, *J Mol Biol 319*, 209-227.
6. Shen, Y., Delaglio, F., Cornilescu, G., and Bax, A. (2009) TALOS^{+}: a hybrid method for predicting protein backbone torsion angles from NMR chemical shifts, *J Biomol NMR 44*, 213-223.
7. Schwieters, C. D., Kuszewski, J. J., Tjandra, N., and Clore, G. M. (2003) The Xplor-NIH NMR molecular structure determination package, *J Magn Reson 160*, 65-73.
8. Linge, J. P., Williams, M. A., Spronk, C. A., Bonvin, A. M., and Nilges, M. (2003)

Refinement of protein structures in explicit solvent, *Proteins 50*, 496-506.
9. Fiedler, B., Zhang, M. M., Buczek, O., Azam, L., Bulaj, G., Norton, R. S., Olivera, B. M., and Yoshikami, D. (2008) Specificity, affinity and efficacy of ι-conotoxin RXIA, an agonist of voltage-gated sodium channels $Na_V1.2$, 1.6 and 1.7, *Biochem Pharmacol 75*, 2334-2344.
10. Hille, B. (2001) *Ion channels of excitable membranes*, Third Edition, Sinauer Associates, Inc., Sunderland, MA.